

A note on variational discretization of elliptic Neumann
boundary control*

by

Michael Hinze¹ and Ulrich Matthes²

¹ Schwerpunkt Optimierung und Approximation, Universität Hamburg,
Bundesstraße 55, 20146 Hamburg, Germany

² Institut für Numerische Mathematik,
TU Dresden, Zellescher Weg 12-14, 01062 Dresden, Germany

Abstract: We consider variational discretization of Neumann-type elliptic optimal control problems with constraints on the control. In this approach the cost functional is approximated by a sequence of functionals, which are obtained by discretizing the state equation with the help of linear finite elements. The control variable is not discretized. Error bounds for control and state are obtained both in two and three space dimensions. Finally, we discuss some implementation issues of a generalized Newton method applied to the numerical solution of the problem class under consideration.

Keywords: elliptic optimal control problem, error estimates, Neumann boundary control, variational discretization.

1. Introduction

Let $\Omega \subset \mathbb{R}^d$ ($d = 2, 3$) be a bounded domain with sufficiently smooth or convex, polygonal boundary $\Gamma := \partial\Omega$. In this note, we are interested in the following control problem:

$$\begin{aligned} \min_{w \in U} J(w) &= \frac{1}{2} \int_{\Omega} |\mathcal{G}(Bw) - y_0|^2 + \frac{\alpha}{2} \|w\|_U^2 \\ \text{subject to } w &\in U_{ad}. \end{aligned} \tag{1}$$

We suppose that $\alpha > 0$ is given. Further, $U := L^2(\Gamma)$ denotes a Hilbert space of controls which we identify with its dual, $B : U \rightarrow (H^1(\Omega))'$ defined by

$$Bu(\cdot) = \int_{\Gamma} u \gamma_0(\cdot) d\Gamma$$

*Submitted: December 2008; Accepted: June 2009.

is the linear and continuous control operator, and $U_{ad} \subseteq U$ denotes the closed, convex set of admissible controls. Furthermore, for given $f \in (H^1(\Omega))'$ the function $\mathcal{G}(f)$ denotes the unique weak solution $y \in H^1(\Omega)$ to the elliptic boundary value problem

$$a(y, v) = \langle f, v \rangle \quad \forall v \in H^1(\Omega). \quad (2)$$

Here, $\langle \cdot, \cdot \rangle$ denotes the dual pairing of $H^1(\Omega)'$ and $H^1(\Omega)$, the bilinear form a is defined by

$$a(y, v) := \int_{\Omega} \left(\sum_{i,j=1}^d a_{ij}(x) y_{x_i} v_{x_j} + \sum_{i=1}^d b_i(x) y_{x_i} v + c(x) y v \right) dx,$$

where we assume that the coefficients $a_{i,j}$, b_i and c are sufficiently smooth and chosen such that the form is H^1 -coercive with constant $c_1 > 0$.

Now, it is not hard to prove that problem (1) admits a unique solution $u \in U_{ad}$. Moreover, there exists a function $p \in H^1(\Omega)$ which, together with $y = \mathcal{G}(Bu)$, satisfies

$$a(v, p) = \int_{\Omega} (y - y_0) v \quad \forall v \in H^1(\Omega) \quad (3)$$

$$(B^*p + \alpha u, q - u)_U \geq 0 \quad \text{for all } q \in U_{ad}. \quad (4)$$

A finite element analysis for general semilinear elliptic Neumann boundary control problems on two-dimensional polygonal convex domains is provided by Casas and Mateos (2008). Among other things they prove $\|u - u_h\|_{L^2(\Gamma)} = o(h)(h \rightarrow 0)$ for a piecewise linear, continuous finite element approximation u_h of u , and, for cost functionals with quadratic structure in the control part, $\|u - u_h\|_{L^2(\Gamma)} = O(h^{3/2-\epsilon})(h \rightarrow 0)$ for the variational discretization u_h , where in both cases $u \in U_{ad}$ denotes a solution to the corresponding optimal control problem.

Here we provide results for two- and three-dimensional domains and provide error estimates in $L^2(\Gamma)$ and $L^\infty(\Gamma)$ for variational discretizations of problem (1). We use a general proof technique which differs from that applied in Casas and Mateos (2008). We concentrate on linear-quadratic optimal control problems since the essential nonlinearity from the point of view of optimization is introduced through the constraint $u \in U_{ad}$ in terms of the orthogonal projection associated with this constraint.

Let us comment on further approaches that tackle optimization problems for PDEs with constrained boundary controls. In Casas, Mateos and Tröltzsch (2005) a problem similar to that of Casas and Mateos (2008) is studied and piecewise constant approximations for the control are investigated. In Casas and Raymond (2007), the Dirichlet boundary control for semilinear elliptic control problems is considered for convex polygonal domains in two dimensions. In

Vexler (2007) h^2 convergence for superpositions of smooth Dirichlet boundary control actions for linear-quadratic optimal control problems is proven. Finally, Dirichlet boundary control for two- and three-dimensional smooth domains is considered in Deckelnick, Günther and Hinze (2008), where also superconvergence properties of finite element approximations are exploited for achieving improved error bounds on finite element meshes exhibiting certain mesh regularity properties.

The rest of the paper is organized as follows: In Section 2 we collect basic results on (1). In Section 3 we present the finite element analysis of problem (1). Among other aspects we show

$$\|u - u_h\|_{L^2(\Gamma)} \sim \|p - p^h(u)\|_{L^2(\Gamma)} + \|y - y^h(u)\|$$

where u_h denotes the unique solution to (6) and y^h, p^h denote finite element approximations to the optimal state y and to the adjoint state p associated to u , respectively. Furthermore, in Theorem 2 we prove the (to the author's knowledge new) uniform estimate

$$\|u - u_h\|_{L^\infty(\Gamma)} \leq C \{ \|p - p^h\|_{L^\infty(\Gamma)} + \gamma(h) \|y - y^h\| \},$$

where $\gamma(h) = |\ln h|$ for $d = 2$, and $\gamma(h) = h^{-1/2}$ for $d = 3$. In Section 5 we describe the numerical implementation of the semi-smooth Newton algorithm for the problem class under consideration and present numerical results which confirm our theoretical findings. Semi-smooth Newton methods for elliptic and parabolic variational discrete control problems are investigated in Hinze, Vierling (2008).

2. The continuous problem

Since problem (1) is convex, it admits a unique solution $u \in U_{ad}$ with unique associated state $y = \mathcal{G}(Bu)$ and unique adjoint p . Crucial for the finite element analysis is the regularity of the involved state, adjoint, and control. From here onwards let us assume that $U_{ad} = \{v \in L^2(\Gamma); a \leq v \leq b \text{ a.e. in } \Gamma\}$, where for simplicity $a < b$ denote constants (or sufficiently smooth, bounded functions, which on the discrete level have to be suitably approximated). From (4) we deduce that u satisfies

$$u = P_{U_{ad}} \left(-\frac{1}{\alpha} B^* p \right), \quad (5)$$

where B^* denotes the adjoint of B , and in the present setting coincides with the trace operator, and the action of the orthogonal projection $P_{U_{ad}} : U \rightarrow U_{ad}$ is given by

$$P_{U_{ad}}(f)(x) = \max\{a, \min\{f(x), b\}\}.$$

Since \max, \min are Lipschitz continuous functions we may at best expect Lipschitz continuity of $P_{U_{ad}}(f)$, regardless of how smooth the function f is. Thus, a bootstrapping argument at best yields $u \in W^{1,\infty}(\Gamma)$ with corresponding state $y \in W^{2,s}(\Omega)$ and adjoint $p \in W^{4,s}(\Omega)$ for all $1 \leq s < \infty$. In the case of a convex polygonal domain both the regularity of y and p is further restricted to $y \in W^{2,s_0}(\Omega)$ for some $d \leq s_0 < \infty$, and $p \in W^{2,s}(\Omega)$ for some $d \leq s < \infty$.

3. Finite element discretization and error analysis for (1)

Let \mathcal{T}_h be a triangulation of Ω with maximum mesh size $h := \max_{T \in \mathcal{T}_h} \text{diam}(T)$ and vertices x_1, \dots, x_m . We suppose that $\bar{\Omega}$ is the union of the elements of \mathcal{T}_h , so that element edges lying on the boundary are curved, see e.g. Bernardi (1989). In addition, we assume that the triangulation is quasi-uniform in the sense that there exists a constant $\kappa > 0$ (independent of h) such that each $T \in \mathcal{T}_h$ is contained in a ball of radius $\kappa^{-1}h$ and contains a ball of radius κh . Let us define the space of linear finite elements,

$$X_h := \{v_h \in C^0(\bar{\Omega}) \mid v_h \text{ is a linear polynomial on each } T \in \mathcal{T}_h\}$$

with the appropriate modification for boundary elements.

In what follows it is convenient to introduce a discrete approximation of the operator \mathcal{G} . In fact, for a given function $f \in H^1(\Omega)'$ we denote by $z_h = \mathcal{G}_h(f) \in X_h$ the solution of the discrete Neumann problem

$$a(z_h, v_h) = \langle f, v_h \rangle \text{ for all } v_h \in X_h.$$

Problem (1) is now approximated by the following sequence of control problems depending on the mesh parameter h :

$$\min_{u \in U_{ad}} J_h(u) := \frac{1}{2} \int_{\Omega} |\mathcal{G}_h(Bu) - y_0|^2 + \frac{\alpha}{2} \|u\|_U^2. \quad (6)$$

Problem (6) represents a convex infinite-dimensional optimization problem of a similar structure as problem (1). It admits a unique solution $u_h \in U_{ad}$ with corresponding state $y_h \in X_h$. Furthermore, in accordance with problem (1), there exists a unique function $p_h \in X_h$ satisfying

$$a(v_h, p_h) = \int_{\Omega} (y_h - y_0)v_h \text{ for all } v_h \in X_h, \text{ and} \quad (7)$$

$$(\alpha u_h + B^* p_h, v - u_h)_U \geq 0 \text{ for all } v \in U_{ad}. \quad (8)$$

Moreover

$$u_h = P_{U_{ad}} \left(-\frac{1}{\alpha} B^* p_h \right). \quad (9)$$

We note that the control is not discretized in (6), which is reflected by the appearance of the orthogonal projector $P_{U_{ad}}$ in (9), compare Hinze (2005) and Hinze et al. (2009) for a more detailed discussion of this discretization approach.

Next we prove a general error estimate in h .

THEOREM 1 *Let u denote the solution of (1) with $y = \mathcal{G}(Bu)$, and u_h the solution to (6) with $y_h = \mathcal{G}_h(Bu_h)$. Then*

$$\alpha \|u - u_h\|_U^2 + \|y - y_h\|^2 \leq C_\alpha \|p - p^h\|_{L^2(\Gamma)}^2 + \|y - y^h\|^2, \quad (10)$$

where y^h, p^h denote the unique solutions to $a(y^h, v_h) = \langle Bu, v_h \rangle$, and $a(v_h, p^h) = \int_\Omega (y - y_0)v_h$ for all $v_h \in X_h$.

Proof. We use u_h as test function in (4), u as test function in (7) and add the resulting variational inequalities. This yields

$$\begin{aligned} \alpha \|u - u_h\|_U^2 &\leq \langle B(u_h - u), p - p_h \rangle = \\ &= \langle B(u_h - u), p - p^h \rangle + \langle B(u_h - u), p^h - p_h \rangle \leq \\ &\leq \|B^*(p - p^h)\|_U \|u - u_h\|_U + a(y_h - y^h, p^h - p_h) = \\ &= \|B^*(p - p^h)\|_U \|u - u_h\|_U + \int_\Omega (y - y_h)(y_h - y^h) \leq \\ &\leq \|B^*(p - p^h)\|_U \|u - u_h\|_U - \frac{1}{2} \|y - y_h\|^2 + \frac{1}{2} \|y - y^h\|^2. \end{aligned}$$

Since B^* coincides with the trace operator, we obtain, with the help of Young's inequality

$$\alpha \|u - u_h\|_U^2 + \|y - y_h\|^2 \leq C_\alpha \|p - p^h\|_{L^2(\Gamma)}^2 + \|y - y^h\|^2.$$

This completes the proof. \blacksquare

Next we prove L^∞ error estimates for the optimal controls.

THEOREM 2 *Let u denote the solution of (1) with $y = \mathcal{G}(Bu)$, and u_h the solution to (6) with $y_h = \mathcal{G}_h(Bu_h)$. Then*

$$\|u - u_h\|_{L^\infty(\Gamma)} \leq C \{ \|p - p^h\|_{L^\infty(\Gamma)} + \gamma(h) \|y - y^h\| \}, \quad (11)$$

where $\gamma(h) = |\ln h|$ for $d = 2$, and $\gamma(h) = h^{-1/2}$ for $d = 3$.

Proof. With the help of (5), (9) we obtain

$$\begin{aligned} \|u - u_h\|_{L^\infty(\Gamma)} &= \|P_{U_{ad}}(-\frac{1}{\alpha} B^* p) - P_{U_{ad}}(-\frac{1}{\alpha} B^* p_h)\|_{L^\infty(\Gamma)} \leq \\ &\leq \frac{1}{\alpha} \|p - p_h\|_{L^\infty(\Gamma)} \leq \frac{1}{\alpha} \|p - p^h\|_{L^\infty(\Gamma)} + \frac{1}{\alpha} \|p^h - p_h\|_{L^\infty(\Gamma)} \leq \\ &\leq \frac{1}{\alpha} \|p - p^h\|_{L^\infty(\Gamma)} + \gamma(h) \|p^h - p_h\|_{H^1(\Omega)}, \end{aligned}$$

where $\gamma(h) = |\ln h|$ for $d = 2$, see Xu and Zou (1998) and $\gamma(h) = h^{-1/2}$ for $d = 3$. We proceed with estimating $\|p^h - p_h\|_{H^1(\Omega)}$ according to

$$\|p^h - p_h\|_{H^1(\Omega)}^2 \leq C a(p^h - p_h, p^h - p_h) \leq C \|p^h - p_h\| \|y - y_h\|.$$

This completes the proof. \blacksquare

From the estimates (10) and (11) we deduce that the approximation quality of the control is steered by the approximation quality of finite element solutions y^h to the state y , and by the finite element approximation p^h of the adjoint p .

Let us consider some examples.

EXAMPLE 1

1. Let us consider the situation of Casas and Mateos (2008), Section 5.6, where Ω is a two-dimensional convex polygonal domain, i.e. $d = 2$. Further let $y_0 \in L^2(\Omega)$. Then $y, p \in H^2(\Omega)$, so that by Casas and Mateos (2008), Theorem 4.1, we have $\|y - y^h\| \leq Ch^2$ and $\|p - p^h\|_{L^2(\Gamma)} \leq h^{3/2}$. Thus, (10) directly yields

$$\|u - u_h\|_{L^2(\Gamma)} \leq Ch^{3/2}.$$

2. Let us consider a smooth, bounded two- or three-dimensional domain Ω and let the approximation properties A1-A4 of Schatz (1998) be satisfied. Bootstrapping yields at least $y \in H^2(\Omega)$ and $p \in H^4(\Omega) \hookrightarrow W^{2,\infty}(\Omega)$ for $d < 4$. Thus we deduce from Schatz (1998), Theorem 2.2,

$$\|p - p^h\|_{\infty} \leq Ch^{2-\frac{d}{q}} |\log h| \|p\|_{W^{2,q}} \text{ for all } d \leq q \leq \infty,$$

compare also Deckelnick and Hinze (2007), Lemma 3.4, and again $\|y - y^h\| \leq Ch^2$. Thus, (11) directly yields

$$\|u - u_h\|_{L^\infty(\Gamma)} \leq C \left\{ h^{2-\frac{d}{q}} |\log h| + \gamma(h)h^2 \right\} \text{ for all } d \leq q \leq \infty.$$

We should note that when using finite element approximations defined over partitions formed of simplexes one has to consider also an error induced by boundary approximations. However, locally, for small enough gridsizes, the smooth boundary may be parameterized as a graph over the faces of the corresponding simplex. For smooth boundaries the difference of the areas of the face and the corresponding graph is bounded by the square of the gridsize, so that error estimates of the same quality as in this example also hold for the accordingly transformed continuous solution, see Deckelnick, Günther and Hinze (2008).

4. Semismooth Newton algorithm

To solve problem (6) numerically we apply a semi-smooth Newton algorithm to the equation

$$G(u) := u - P_{U_{ad}} \left(-\frac{1}{\alpha} B^* p_h(u) \right) = 0 \text{ in } U, \quad (12)$$

where for given $u \in U$ with associated discrete state $y_h(u)$ the function $p_h(u)$ solves (7). It follows from (5) that this equation in our setting admits the unique

solution $u_h \in U_{ad}$ of problem (6). Moreover, it directly follows with the results of Hintermüller, Ito and Kunisch (2003) and Ulbrich (2003) that G is semi-smooth in the sense that

$$\sup_{M \in \partial G(u+s)} \|G(u+s) - G(u) - Ms\|_U = o(\|s\|_U) \text{ as } \|s\|_U \rightarrow 0,$$

where

$$\partial G(u) := \left\{ I + D(u) \left(\frac{1}{\alpha} B^* p'_h(u) \right) \right\}$$

$$\text{with } D(u)(x) = \begin{cases} 0, & \text{if } -\frac{1}{\alpha} B^* p_h(u)(x) \notin [a, b] \\ \in [0, 1], & \text{if } -\frac{1}{\alpha} B^* p_h(u)(x) \in \{a, b\} \\ 1, & \text{if } -\frac{1}{\alpha} B^* p_h(u)(x) \in (a, b) \end{cases}$$

denotes the generalized differential. With $g \equiv g(u)$ denoting the indicator function of the inactive set $\mathcal{I}(u) := \{x \in \Gamma; -\frac{1}{\alpha} B^* p_h(u)(x) \in (a, b)\}$ we set

$$G'(u) := I + \frac{1}{\alpha} g B^* p'_h(u) \in \partial G(u).$$

It follows from the considerations related to (16) that $G'(u)$ is bounded invertible, since $p'_h(u) = S_h^* S_h B$ with S_h denoting the finite element solution operator. Thus, $B^* p'_h(u) = B^* S_h^* S_h B$ is positive semi-definite on U .

We are now in the position to formulate

ALGORITHM 1 *Semi-smooth Newton algorithm*

Choose $u \in U$

While $G(u) \neq 0$ solve

$$G'(u)u^{new} = G'(u)u - G(u) \tag{13}$$

for u^{new} and set $u = u^{new}$.

We emphasize that this algorithm works in the infinite-dimensional space U so that it is not obvious that this algorithm is numerically implementable. For a related discussion we refer to Hinze (2005).

Using

$$\beta := (I - g)\text{bounds} \equiv \begin{cases} a, & \text{if } -\frac{1}{\alpha} B^* p_h(u) < a \\ b, & \text{if } -\frac{1}{\alpha} B^* p_h(u) > b \\ 0, & \text{else} \end{cases}$$

a short calculation shows that the Newton equation (13) can be rewritten in the form

$$u^{new} = \text{bounds on } \mathcal{A}(u) := \Gamma \setminus \mathcal{I}(u), \text{ and} \tag{14}$$

$$(\alpha g I + g B^* S_h^* S_h B g) u^{new} = -g B^* (S_h^* y_0 - S_h^* S_h B \beta). \tag{15}$$

We solve the equation

$$(\alpha gI + gB^* S_h^* S_h B g) u^{new} = -gB^*(S_h^* y_0 - S_h^* S_h B \beta)$$

with a conjugate gradient method. This is feasible since for given $u \in U$ the operator $\mathcal{E}_I^*(\alpha I + B^* S_h^* S_h B) \mathcal{E}_I$ is positive definite on $L^2(\mathcal{I}(u))$, where the function $\mathcal{E}_I f \in L^2(\Gamma)$ denotes the extension-by-zero to Γ of functions $f \in L^2(\mathcal{I}(u))$, and \mathcal{E}_I^* denotes its adjoint whose action for $s \in L^2(\Gamma)$ is given by $\mathcal{E}_I^* s = (gs)|_{\mathcal{I}(u)}$. Thus, formally solving (15),(14) corresponds to solving

$$\mathcal{E}_I^*(\alpha I + B^* S_h^* S_h B) \mathcal{E}_I u_I^{new} = -\mathcal{E}_I^* B^*(S_h^* y_0 - S_h^* S_h B \beta) \quad (16)$$

and then setting $u^{new} = u_I^{new}$ on $\mathcal{I}(u)$, and $u^{new} =$ bounds on $\mathcal{A}(u)$, compare also Hintermüller, Ito and Kunisch (2003), (4.7).

It is now clear from these considerations that the Newton iterates may develop kinks or even jumps along the border of the active set, see the numerical results of the next section. However, it follows from the definition of the active set $\mathcal{A}(u)$ that its border consists of polygons, since we use continuous, piecewise linear ansatz functions for the state. We note that this border, in general, consists of piecewise polynomials of the same degree as that of the finite element ansatz functions, if higher order finite elements are used, compare Hinze et al. (2009). Therefore, Algorithm 1 is numerically implementable, since in every of its iterations only a finite number of degrees of freedom has to be managed, which in the present case of linear finite elements can not exceed $3nv + 2ne$, where nv denotes the number of finite element nodes, and ne the number of finite element edges, see Hinze et al. (2009), Chapter 3 and Hinze (2005) for details. Moreover, the main ingredient of the cg algorithm applied to solve the Newton equation (16) consists in evaluating $\mathcal{E}_I^*(\alpha I + B^* S_h^* S_h B) \mathcal{E}_I f$ for functions $f \in L^2(\mathcal{I}(u))$. From the definitions of B and S_h it is then clear, which actions have to be performed for this evaluation.

It is also clear, that only local convergence of the semi-smooth Newton algorithm can be expected, where the convergence radius at the solution depends on the penalization parameter α . For the numerical examples presented in the next section and the considered values of α it is sufficient to use a cascading approach, where linear interpolations of numerical solutions on coarse grids are used as starting values on the next, finer grid. Further details on the semi-smooth Newton methods applied to variationally discretized optimal control problems can be found in Hinze and Vierling (2008), where, in particular, also time-dependent problems are considered and globalization strategies are proposed.

5. Numerical experiments

We consider two numerical examples taken from Casas and Mateos (2008) and compare the results of our numerical approach to the classical approach with

piecewise linear, continuous ansatz functions for the controls taken there. For this purpose we define the experimental order of convergence by

$$eoc = \frac{\log E(h_1) - \log E(h_2)}{\log h_1 - \log h_2},$$

where $E(h)$ denotes an error functional an h the finite element grid size. There holds $eoc \sim \gamma$ if $E(h) \sim h^\gamma$.

In the examples investigated later an additional nonlinear function $e_u : \Gamma \rightarrow \mathbb{R}$ appears, which necessitates the projection of nonlinear functions in the form

$$u = P_{U_{ad}}(-\frac{1}{\alpha}(B^*p_h + e_u)).$$

For the integration over the boundary control with kinks, we divide the boundary, additionally to the division by the FEM discretization at the positions of the kinks. The kinks occur at prescribed points in e_u and at the intersections with the constraints. The latter are calculated with the Pegasus method (an improved regula-falsi method), Dowell and Jarratt (1972), because of the nonlinearity in e_u .

5.1. Example 1

Taken from Casas and Mateos (2008), Section 7.1 (see also Casas, Mateos and Tröltzsch, 2005), this example reads

$$\begin{aligned} \min \hat{J}(u) = & \frac{1}{2} \int_{\Omega} (y_u(x) - y_{\Omega})^2 dx + \frac{\alpha}{2} \int_{\Gamma} u(x)^2 dx + \int_{\Gamma} e_u(x)u(x)dx + \\ & + \int_{\Gamma} e_y(x)y_u(x)dx \end{aligned}$$

subject to $u \in U_{ad} = \{u \in L^2; 0 \leq u(x) \leq 1 \text{ a.e. } x \in \Gamma\}$, where y_u solves

$$\begin{aligned} -\Delta y_u(x) + c(x)y_u(x) &= e_1(x) & \text{in } \Omega, \\ \partial_{\nu} y_u(x) + y_u(x) &= e_2(x) + u(x) & \text{on } \Gamma. \end{aligned}$$

Here, $\Omega = (0, 1)^2$, $\alpha = 1$, $c(x) = 1 + x_1^2 - x_2^2$, $e_y(x) = 1$, $y_{\Omega}(x) = x_1^2 + x_1x_2$, $e_1(x) = -2 + (1 + x_1^2 - x_2^2)(1 + 2x_1^2 + x_1x_2 - x_2^2)$,

$$e_u(x) = \begin{cases} -1 - x_1^3 & \text{on } \Gamma_1 \\ -1 - \min \left\{ \begin{array}{l} 8(x_2 - 0.5)^2 + 0.58 \\ 1 - 16x_2(x_2 - y_1^*)(x_2 - y_2^*)(x_2 - 1) \end{array} \right\} & \text{on } \Gamma_2 \\ -1 - x_1^2 & \text{on } \Gamma_3 \\ -1 + x_2(1 - x_2) & \text{on } \Gamma_4, \end{cases}$$

with $y_1^* = \frac{1}{2} - \frac{\sqrt{21}}{20}$ and $y_2^* = \frac{1}{2} + \frac{\sqrt{21}}{20}$. Further

$$e_2(x) = \begin{cases} 1 - x_1 + 2x_1^2 - x_1^3 & \text{on } \Gamma_1 \\ 7 + 2x_2 - x_2^2 - \min\{8(x_2 - 0.5)^2 + 0.58, 1\} & \text{on } \Gamma_2 \\ -2 + 2x_1 + x_1^2 & \text{on } \Gamma_3 \\ 1 - x_2 - x_2^2 & \text{on } \Gamma_4 \end{cases}$$

where Γ_1 to Γ_4 are the four edges of the unit square, numbered counterclockwise, starting with the bottom edge. The adjoint equation is given by

$$\begin{aligned} -\Delta\phi(x) + c(x)\phi(x) &= y_u(x) - y_\Omega(x) & \text{in } \Omega \\ \partial_\nu\phi(x) + \phi(x) &= e_y(x) & \text{on } \Gamma. \end{aligned}$$

An easy calculation shows that the optimal solution is given by

$$\bar{u}(x) = \begin{cases} x_1^3 & \text{on } \Gamma_1 \\ \min\{8(x_2 - 0.5)^2 + 0.58, 1\} & \text{on } \Gamma_2 \\ x_1^2 & \text{on } \Gamma_3 \\ 0 & \text{on } \Gamma_4, \end{cases}$$

with corresponding state $\bar{y}(x) = 1 + 2x_1^2 + x_1x_2 - x_2^2$ and adjoint state $\bar{\phi}(x) = 1$.

We note that in the numerical approach for this example (12) has to be replaced by

$$G(u) = u - P_{U_{ad}}\left(-\frac{1}{\alpha}(B^*p_h + e_u)\right)$$

so that special attention has to be paid, caused by the nonlinearity of e_u , when evaluating $P_{U_{ad}}\left(-\frac{1}{\alpha}(B^*p_h(u) + e_u)\right)$ for given u .

The errors and eocs are shown in Table 1 for the Casas-Mateos-ansatz and the variational discretization, respectively. The eoc of the numerical experiments of Casas and Mateos is calculated from tables of Casas and Mateos (2008). The eoc of the numerical experiments of Casas and Mateos is 1.5 and about 1.0 for the L^2 and L^∞ norm, respectively. The eoc is 2 for our approach. This is better than expected by Example 1 (1), in Section 3. However, this may be caused by the special regularity of the continuous solution and the domain. The latter is polygonal, but forms the limit case in regularity theory for elliptic domains with corners, so that also the estimate of Example 1 (2), in Section 3 may apply. This would coincide with our numerical results. We further note that already the errors on the coarsest mesh for $h = 1$ are smaller in our approach than those for $h = 2^{-4}$ or $h = 2^{-6}$ in the conventional Casas-Mateos-ansatz.

The Newton iteration is terminated if $\|G(u^i)\|/\|G(u^0)\| \leq 10^{-5}$ and $\|u^i - u^{i-1}\|/\max(\|u^i\|, \|u^{i-1}\|) \leq 10^{-5}$ holds. The inner cg iteration is terminated if $\|r\| \leq \frac{10^{-4}}{i} \min\{1, \|G(u^i)\|/\|G(u^i)\|/\|G(u^0)\|\}$ holds with r denoting the current residuum of the Newton system.

In Fig. 1 the optimal control, together with the error for $h = 0.5$ and the finite element grid, is shown.

Table 1. Errors in u for the linear example

h	Casas and Mateos		This paper		Casas and Mateos		This paper	
	$E_{u_{L^2}}$	$E_{u_{L^\infty}}$	$E_{u_{L^2}}$	$E_{u_{L^\infty}}$	$eoc_{u_{L^2}}$	$eoc_{u_{L^\infty}}$	$eoc_{u_{L^2}}$	$eoc_{u_{L^\infty}}$
2^{-0}	-	-	6.67e-3	5.03e-3	-	-	-	-
2^{-1}	-	-	2.27e-3	2.14e-3	-	-	1.55	1.23
2^{-2}	-	-	6.28e-4	5.72e-4	-	-	1.86	1.90
2^{-3}	-	-	1.62e-4	1.47e-4	-	-	1.95	1.96
2^{-4}	8.5e-3	4.1e-2	4.10e-5	3.73e-5	-	-	1.98	1.98
2^{-5}	3.0e-3	1.5e-2	1.03e-5	9.34e-6	1.5	1.5	1.99	2.00
2^{-6}	1.1e-3	1.1e-2	2.58e-6	2.34e-6	1.4	0.4	2.00	2.00
2^{-7}	3.7e-4	3.8e-3	6.44e-7	5.84e-7	1.6	1.5	2.00	2.00
2^{-8}	1.4e-4	2.7e-3	1.61e-7	1.46e-7	1.4	0.5	2.00	2.00
2^{-9}	-	-	4.03e-8	3.65e-8	-	-	2.00	2.00
2^{-10}	-	-	1.00e-8	9.09e-9	-	-	2.01	2.01

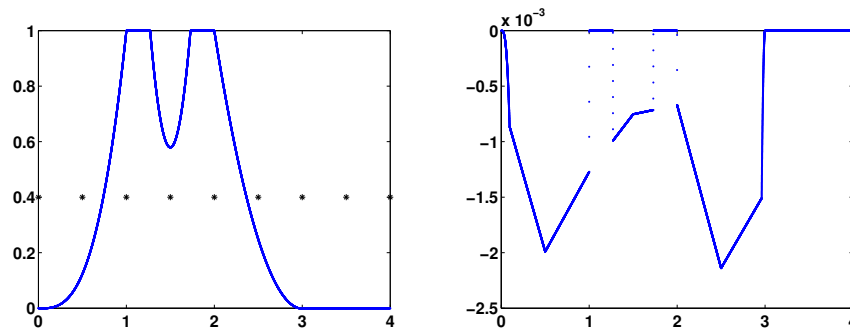


Figure 1. Optimal control u left, error in u right, both for $h = 0.5$.

5.2. Example 2

Taken from Casas and Mateos (2008), Section 7.2 (compare also the semilinear example in Casas, Mateos and Tröltzsch, 2005), this example contains a semilinear state equation instead of a linear one. It reads

$$\begin{aligned} \min \hat{J}(u) = & \frac{1}{2} \int_{\Omega} (y_u(x) - y_{\Omega})^2 dx + \frac{\alpha}{2} \int_{\Gamma} u(x)^2 dx + \int_{\Gamma} e_u(x) u(x) dx + \\ & + \int_{\Gamma} e_y(x) y_u(x) dx \end{aligned}$$

subject to $u \in U_{ad} = \{u \in L^2; 0 \leq u(x) \leq 1 \text{ a.e. } x \in \Gamma\}$, where y_u satisfies the semilinear equation

$$\begin{aligned} -\Delta y_u(x) + c(x)y_u(x) &= e_1(x) && \text{in } \Omega \\ \partial_\nu y_u(x) + y_u(x) &= e_2(x) + u(x) - y(x)^2 && \text{on } \Gamma. \end{aligned}$$

Here, $\Omega = (0, 1)^2$, $\alpha = 1$, $c(x) = x_2^2 + x_1x_2$, $e_y(x) = -3 - 2x_1^2 - 2x_1x_2$, $y_\Omega(x) = 1 + (x_1 + x_2)^2$, $e_1(x) = -2 + (1 + x_1^2 + x_1x_2)(x_2^2 + x_1x_2)$,

$$e_u(x) = \begin{cases} 1 - x_1^3 & \text{on } \Gamma_1 \\ 1 - \min \left\{ \begin{array}{l} 8(x_2 - 0.5)^2 + 0.58 \\ 1 - 16x_2(x_2 - y_1^*)(x_2 - y_2^*)(x_2 - 1) \end{array} \right\} & \text{on } \Gamma_2 \\ 1 - x_1^2 & \text{on } \Gamma_3 \\ 1 + x_2(1 - x_2) & \text{on } \Gamma_4, \end{cases}$$

with $y_1^* = \frac{1}{2} - \frac{\sqrt{21}}{20}$ and $y_2^* = \frac{1}{2} + \frac{\sqrt{21}}{20}$. Furthermore,

$$e_2(x) = \begin{cases} 2 - x_1 + 3x_1^2 - x_1^3 + x_1^4 & \text{on } \Gamma_1 \\ 8 + 6x_2 + x_2^2 - \min \{8(x_2 - 0.5)^2 + 0.58, 1\} & \text{on } \Gamma_2 \\ 2 + 4x_1 + 3x_1^2 + 2x_1^3 + x_1^4 & \text{on } \Gamma_3 \\ 2 - x_2 & \text{on } \Gamma_4, \end{cases}$$

The adjoint equation is given by

$$\begin{aligned} -\Delta \phi(x) + c(x)\phi(x) &= y_u(x) - y_\Omega(x) && \text{in } \Omega \\ \partial_\nu \phi(x) + \phi(x) &= e_y(x) - 2y(x)\phi(x) && \text{on } \Gamma. \end{aligned}$$

Again a short calculation shows that

$$\bar{u}(x) = \begin{cases} x_1^3 & \text{on } \Gamma_1 \\ \min \{8(x_2 - 0.5)^2 + 0.58, 1\} & \text{on } \Gamma_2 \\ x_1^2 & \text{on } \Gamma_3 \\ 0 & \text{on } \Gamma_4 \end{cases}$$

is the optimal control with corresponding optimal state $\bar{y}(x) = 1 + x_1^2 + x_1x_2$ and adjoint $\bar{\phi}(x) = -1$.

For the numerical solution of the present example again a semi-smooth Newton method is applied. Since we are dealing with nonlinear state equations, the determination of u^{new} in (15) has to be replaced by

$$\begin{aligned} (\alpha gI + gB^* p'_h(u)g)u^{new} &= -gB^*(p_h(u) - p'_h(u)(u - \beta)), \\ \text{and } u^{new} &= \text{bounds on } \Omega \setminus \mathcal{I}(u). \end{aligned}$$

The numerical results are very similar to those of the previous example. This is due to the fact that the nonlinearity in the state equation is monotone.

The errors and eocs for the present example are shown in Table 2 for the Casas-Mateos-ansatz and the variational discretization, respectively. The eoc of the numerical experiments of Casas and Mateos is calculated again from their reference. The eoc of the numerical experiments of Casas and Mateos is 1.5 and about 1.0 for the L^2 and L^∞ norms, respectively. The eoc is 2 for our approach. This again is better than expected by Example 1, 1, but the same arguments as used in the previous example may justify also convergence order 2. We further note that also for this example already the errors on the coarsest mesh for $h = 1$ are smaller in our approach than than those for $h = 2^{-4}$ in the conventional Casas-Mateos-ansatz.

The termination conditions are the same as in the previous example.

In Fig. 2 the optimal control, together with the error for $h = 0.5$ and the finite element grid, is shown.

Table 2. Errors in u for the semilinear example

h	Casas and Mateos		This paper		Casas and Mateos		This paper	
	$E_{u_{L^2}}$	$E_{u_{L^\infty}}$	$E_{u_{L^2}}$	$E_{u_{L^\infty}}$	$eoc_{u_{L^2}}$	$eoc_{u_{L^\infty}}$	$eoc_{u_{L^2}}$	$eoc_{u_{L^\infty}}$
2^{-0}	-	-	1.13e-2	1.83e-2	-	-	-	-
2^{-1}	-	-	4.72e-3	6.43e-3	-	-	1.26	1.51
2^{-2}	-	-	1.33e-3	2.19e-3	-	-	1.82	1.55
2^{-3}	-	-	3.45e-4	6.69e-4	-	-	1.95	1.71
2^{-4}	8.5e-3	4.1e-2	8.75e-5	1.89e-4	-	-	1.98	1.82
2^{-5}	3.0e-3	1.5e-2	2.20e-5	5.11e-5	1.5	1.5	1.99	1.89
2^{-6}	1.1e-3	1.1e-2	5.50e-6	1.33e-5	1.4	0.4	2.00	1.94
2^{-7}	3.8e-4	3.8e-3	1.38e-6	3.42e-6	1.5	1.5	2.00	1.96
2^{-8}	1.4e-4	2.7e-3	3.44e-7	8.66e-7	1.4	0.5	2.00	1.98
2^{-9}	-	-	8.61e-8	2.18e-7	-	-	2.00	1.99
2^{-10}	-	-	2.15e-8	5.47e-8	-	-	2.00	1.99

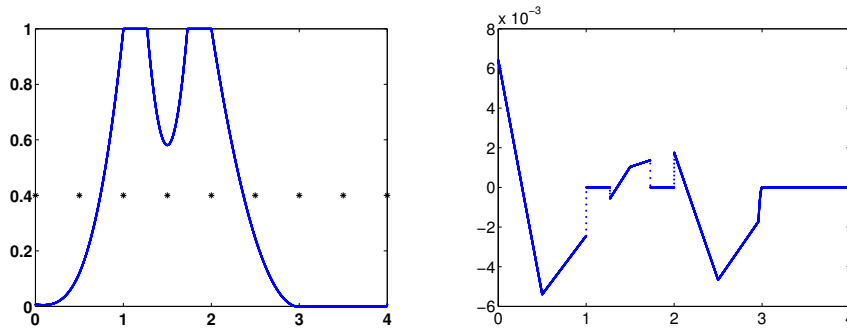


Figure 2. Optimal control u left, error in u right, both for $h = 0.5$

Acknowledgements

The first author gratefully acknowledges the support of the DFG Priority Program 1253 entitled *Optimization With Partial Differential Equations*.

References

- BERNARDI, C. (1989) Optimal Finite-Element Interpolation on Curved Domains. *SIAM J. Numer. Anal.* **26** (5), 1212-1240.
- CASAS, E. and RAYMOND, J.P. (2007) Error Estimates for the Numerical Approximation of Dirichlet Boundary Control for Semilinear Elliptic Equations. *SIAM J. Control Optim.* **45**, 1586-1611.
- CASAS, E. and MATEOS, M. (2008) Error Estimates for the Numerical Approximation of Neumann Control Problems. *Comput. Optim. Appl.* **39**, 265-295.
- CASAS, E., MATEOS, M. and TRÖLTZSCH, F. (2005) Error Estimates for the Numerical Approximation of Boundary Semilinear Elliptic Control Problems. *Comput. Optim. Appl.* **31**, 193-220.
- DECKELNICK, K. and HINZE, M. (2007) Convergence of a finite element approximation to a state constrained elliptic control problem. *SIAM J. Numer. Anal.* **45**, 1937-1953.
- DECKELNICK, K., GÜNTHER, A. and HINZE, M. (2008) Finite element approximation of Dirichlet boundary control for elliptic PDEs on two- and three-dimensional curved domains. Preprint No. SPP1253-08-05, DFG Priority Program 1253. To appear in *SIAM J. Contr. Optim.*
- DOWELL, M. and JARRATT, P. (1972) The Pegasus method for computing the root of an equation. *BIT* **12**, 503-508.
- HINTERMÜLLER, M., ITO, K. and KUNISCH, K. (2003) The primal-dual active set method as a semi-smooth Newton method. *SIAM J. Control and Optim.* **13**, 865-888.
- HINZE, M. (2005) A variational discretization concept in control constrained optimization: the linear-quadratic case. *J. Computational Optimization and Applications* **30**, 45-63.
- HINZE, M., PINNAU, R., ULBRICH, M. and ULBRICH, S. (2009) *Optimization with pde constraints. Mathematical Modelling: Theory and Applications* **23**, Springer.
- HINZE, M. and VIERLING, M. (2008) Semi-discretization and semi-smooth Newton methods; implementation, convergence and globalization in pde constrained optimization with control constraints. Preprint, to appear.
- SCHATZ, A.H. (1998) Pointwise error estimates and asymptotic error expansion inequalities for the finite element method on irregular grids. I: Global estimates. *Math. Comput.* **67**, 223, 877-899.
- ULBRICH, M. (2003) Semismooth Newton Methods for Operator Equations in Function Spaces. *SIAM J. Optim.* **13**, 805-841.

-
- VEXLER, B. (2007) Finite Element Approximation of Elliptic Dirichlet Optimal Control Problems. *Numerical Functional Analysis and Optimization* **28**(7-8), 957-973.
- XU, J. and ZOU, J. (1998) Some nonoverlapping domain decomposition methods. *SIAM Rev.* **40**, 857-914.